Manuscript prepared for Biogeosciences Discuss.
with version 2014/09/16 7.15 Copernicus papers of the LaTeX class copernicus.cls.
Date: 19 June 2015

The role of photo- and thermal degradation for CO_2 and CO fluxes in an arid ecosystem

H. van Asperen[1], T. Warneke[1], S. Sabbatini[2], G. Nicolini[2,3], D. Papale[2], and J. Notholt[1]

[1]Institute of Environmental Physics, University of Bremen, Otto-Hahn-Allee 1, Bremen, 28359, Germany
[2]Department for innovation in biological agro-food and forest systems, University of Tuscia, via S. Camillo de Lellis s.n.c., 01100 Viterbo, Italy
[3]EuroMediterranean Center on Climate Changes – Impacts on Agriculture, Forest and Natural Ecosystem Division (IAFENT), 01100 Viterbo, VT, Italy

Correspondence to: H. van Asperen (v_asperen@iup.physik.uni-bremen.de)

Abstract

Recent studies have suggested the potential importance of abiotic degradation in arid ecosystems. In this study, the role of photo- and thermal degradation in ecosystem CO_2 and CO exchange is assessed. A field experiment was performed in Italy using a FTIR-spectrometer coupled to a flux gradient system and to flux chambers. In a laboratory experiment, field samples were exposed to different temperatures and radiation intensities.

No photodegradation-induced CO_2 and CO fluxes of in literature suggested magnitudes were found in the field nor in the laboratory study. In the laboratory, we measured CO_2 and CO fluxes that were derived from thermal degradation. In the field experiment, CO uptake and emission have been measured and are proposed to be a result of biological uptake and abiotic thermal degradation-production.

We suggest that previous studies, addressing direct photodegradation, have overestimated the role of photodegradation and observed fluxes might be due to thermal degradation, which is an indirect effect of radiation. The potential importance of abiotic decomposition in the form of thermal degradation, especially for arid regions, should be considered in future studies.

1 Introduction

CO_2 is the main carbon species being exchanged between biosphere and atmosphere and the most important anthropogenic greenhouse gas. CO is a less abundant non-greenhouse gas but considered important in the climate debate due to its oxidation process with atmospheric OH^- (Stocker et al., 2013). Yearly, terrestrial ecosystems exchange approximately 120 Pg of carbon with the atmosphere (Stocker et al., 2013).

Arid ecosystems account for approximately 40 % of land area and 20 % of the soil carbon pool but are still an unknown factor in climate models (Lal, 2004). In recent studies, the possible importance of abiotic degradation for arid regions, such as photo- and thermal degra-

dation, has been recognized (Austin and Vivanco, 2006; King et al., 2012; Rutledge et al., 2010).

1.1 Ecosystem CO_2 fluxes; photo- and thermal degradation

Photodegradation is the direct breakdown of organic matter by radiation. Photodegradaton is known to be an important pathway in aquatic ecosystems (Zepp et al., 1998). Recently, the possible importance of photodegradation in terrestial ecosystems has been suggested (Austin and Vivanco, 2006; Brandt et al., 2010; Friedlingstein et al., 2006; Rutledge et al., 2010). Photodegradation can play an important role in arid ecosystems, where microbial decomposition is restricted (Austin and Vivanco, 2006; Brandt et al., 2010; Lee et al., 2012; Lin and King, 2014; Throop and Archer, 2009). Rutledge (2010) estimated that in arid ecosystems, 19 % of the annual CO_2 flux is induced by photodegradation and, in dry summer conditions, even 92 % of daytime CO_2 emissions can be attributed to this process.

Photodegradation is attributed to UV as well as visible radiation (Austin and Vivanco, 2006; Brandt et al., 2010; Bruhn et al., 2009). The biochemical mechanisms behind photodegradation-induced carbon fluxes are not clear; it is proposed that solar radiative energy breaks down the bonds of carboxyl, directly producing CO_2 and other gas species (Lee et al., 2012). It has been hypothesized that rates of photodegradation depend on plant and litter tissue type: lignin, one of the most recalcitrant tissue in plant material (to microbial decompostion), is expected to be most sensitive to photodegradation (Austin and Ballaré, 2010; King et al., 2012). However, while studies reporting photodegradation are multiple, recent studies, aiming to further investigate the process, were unable to observe the effects of photodegradation (Kirschbaum et al., 2011; Lambie et al., 2014; Uselman et al., 2011). A reason for this discrepency has not yet been found (Kirschbaum et al., 2011; Lambie et al., 2014; Throop and Archer, 2007; Uselman et al., 2011). It is important to notice that in literature, the term photodegradation is sometimes also used for the indirect effects of radiation on decomposition. One example is microbial faciliation: radiation breaks down organic compounds into smaller molecules, which are then easier degradable for microbes. For a review on studies done on photodegradation, please see King et al. (2012).

A less studied abiotic degradation pathway is thermal degradation, the temperature dependent degradation of carbon in absence of radiation and possibly oxygen (Derendorp et al., 2011; Lee et al., 2012; Schade et al., 1999). However, photodegradation is considered the more dominant abiotic CO_2 producing process (Lee et al., 2012). Besides CO_2, CO and CH_4 are also reported as products of photo- and thermal degradation (Derendorp et al., 2011; Lee et al., 2012; Schade et al., 1999; Tarr et al., 1995; Vigano et al., 2008).

1.2 Ecosystem CO fluxes; photo- and thermal degradation

The role of CO in soils and ecosystems is not well understood. Soils are known for being sources as well as sinks of CO (Conrad, 1996). Most likely, the main cause for soil CO uptake is the oxidation of CO to CO_2 or CH_4 by soil bacteria or soil enzymes (Bartholomew and Alexander, 1979; Conrad, 1996; Ingersoll et al., 1974; Spratt and Hubbard, 1981; Whalen and Reeburgh, 2001; Yonemura et al., 2000). Soil CO consumption is found to be dependent on atmospheric CO concentrations and the consumption rate is usually expressed in deposition velocity: the uptake rate divided by the CO concentration (Conrad and Seiler, 1982; Kisselle et al., 2002).

Soil CO emissions have also been reported and are thought to be of non-biological origin (Conrad and Seiler, 1980, 1982). For example, soil CO emissions were found in peatlands (Funk et al., 1994) and in arid soils (Conrad and Seiler, 1982). Living plants are also known to emit a small amount of CO (Bruhn et al., 2013; Kirchhoff et al., 1990; Tarr et al., 1995). However, senescent plant material has been shown to emit 5 to 10 times more than photosynthesising leaf material (Derendorp et al., 2011; Schade et al., 1999; Tarr et al., 1995). These fluxes, mostly determined in laboratory studies, were attributed to thermal degradation and, to a larger extent, photodegradation (Derendorp et al., 2011; Lee et al., 2012; Schade et al., 1999).

1.3 Measurement of photo- and thermal degradation

Studying photodegradation is difficult due to the multiple (indirect) effects radiation has on total biological decomposition. For example, UV-radiation is known to inhibit microbial processes, to change (senescent) tissue chemistry and to alter the dominating microbial and fungal communities, thereby affecting microbial decomposition rates in both directions (Formánek et al., 2014; Smith et al. , 2010; Williamson et al., 1997; Zepp et al., 1998). Differentiating photodegradation-induced fluxes from biological sources in field experiments can be achieved by comparison of different flux measurement techniques such as Eddy Covariance (EC) measurements vs. flux chamber measurements and/or soil gradient measurements, in that one method does not receive solar radation (Rutledge et al., 2010). This approach requires that the areas or footprints sensed by the different techniques are fully homogeneous, which is not often the case and hard to validate. To study the effects of photodegradation (in field or laboratory), also radiation filters can be used to expose samples to different types or amounts of radiation (Brandt et al., 2010; Lee et al., 2012; Lin and King, 2014).

Studying the role of thermal degradation-induced carbon fluxes is challenging, especially for CO_2 due to the accompanying effect temperature has on microbial decomposition. To study thermal degradation-induced CO_2 production, microbial decomposition should be absent, which can only be achieved in laboratory studies (Lee et al., 2012).

Previous field and laboratory studies on the role of direct or indirect abiotic degradation report very constrasting results (King et al., 2012; Kirschbaum et al., 2011; Lambie et al., 2014; Lee et al., 2012; Rutledge et al., 2010; Uselman et al., 2011). More specific studies are thus needed to better understand this process and its role in the carbon cycle. In this study, we present the results of field and laboratory measurements aimed to evaluate the role of direct photodegradation and thermal degradation in an arid ecosystem.

2 Materials and methods

2.1 Study site

We performed a field experiment in a grassland (IT-Ro4, harvested cropland, approximately 250 m by 450 m, lat 42.37° N, long 11.92° E, 147 m a.s.l.), in the province of Viterbo, Italy. The climate is Mediterranean, with a typical drought period covering approximately 2 months during summer (July–August). Mean annual temperature is 14 °C and annual rainfall is 755 mm. Such climatic characteristics make the site suitable for abiotic degradation studies. The underlying material is Tuff, soil texture is clay loam and soils are classified as Eutric Cambisol. Yearly, the field site is ploughed to a depth of 20 or 50 cm. Just before the experiment, oat and vetch were cultivated. During the experiment, vegetation was not managed and was a mix of invasive species such as *Amaranthus retroflexus*, *Chenopodium* spp., *Conyza Canadensis*, *Artemisia vulgaris*, *Cirsium* spp., *Mercurialis annua* and *Polygonum* spp. The field study was conducted in July–September 2013. At the beginning of the experiment, most vegetation was dried out, however, patches of active vegetation were observed. Temperature and rainfall during measurements were representative for the period (hot and dry) (Fig 2), however, the preceding spring had been cold and rainy in respect to the average.

IT-Ro4 is an experimental site managed by the University of Tuscia (Viterbo). Continuous EC measurements of scalars and energy fluxes are performed (LI-7500 open path analyzer, Licor, Lincoln, Nebraska, USA; Windmaster Pro sonic anenomemeter, Gill, Hampshire, UK) along with meteorological and environmental measurements (CNR-1, Kipp & Zonen, Delft, the Netherlands; soil water content, CS616, Campbell Scientific, North Logan, USA; soil temperature, CS107, Campbell scientific, North Logan, USA; soil heat flux, HFT3 Soil Heat Flux Plate, Campbell scientific, North Logan, USA).

2.2 Instrumentation and set up

The analyzer used in this study is based on a Fourier Transform Infrared (FTIR)-spectrometer (Spectronus, Ecotech), for details on the FTIR-analyzer, see Griffith (2012). A FTIR is capable of measuring air concentrations of CO_2, CH_4, N_2O, CO and $\delta^{13}CO_2$ simultaneously. Before being measured, air samples were dried by a nafion dryer and by a column of magnesium perchlorate. Measurements were corrected for pressure and temperature fluctuations and for cross-sensitivities (Hammer et al., 2013). Background measurements and a calibration routine using two standard gas cylinders were performed weekly. We designed an external manifold box which allowed us to connect the FTIR to a flux gradient (FG) setup and to 2 flux chambers (FC), simultaneously. Both methods provide air concentration data as well as flux data. In this paper, only CO_2 and CO flux data are presented.

2.3 Concentration and flux measurements

FG measurements were performed once per hour and performed at the same location as the EC tower. More information about the FG system can be found in the Supplementary Materials.

For FC measurements, six soil collars ($50\,cm \times 50\,cm$) were inserted to 10 cm depth a week before the start of the experiment. Positions of soil collars were checked for being undisturbed and representative. The two flux chambers (open dynamic chambers, $50\,cm \times 50\,cm \times 50\,cm$, produced by Karlsruhe Institute of Technology, Germany) consisted of a stainless steel frame, UV-transparent acrylic sides (Acryl Glass XT solar, 3mm, UV-transparent) and a vent tube, and were tightened by use of clamps and rubber air strips. Transparency of the acrylic material was measured and reported to be $>$ 90% in the UV and visible wavelength band (280-700 nm). Two fans per flux chamber were continuously running, insuring well-mixed headspace air. Automatic chamber closure (once per hour) was made possible by use of a pneumatic system regulated by the valve manifold box. Air flow from the flux chambers to the FTIR was initiated by a membrane pump placed behind

the measurement cell, set to 1 L min^{-1}. Air flow was measured every 2 min continuously for 20 min in flow mode. Chamber opening and closure was after 4 and 18 min, respectively. Sampling lines from the chambers were of equal size and material and were tested for leaks regularly. Chamber temperatures were recorded by temperature loggers (Voltcraft DL-1181THP). Fluxes were derived from concentration increases after chamber closure, by use of linear regression. Gas fluxes were calculated by:

$$F = \frac{VP}{RST}\frac{\delta C}{\delta t} \quad (1)$$

wherein V is the volume of the chamber (m^3), P the chamber air pressure (Pa), R the gas constant (8.314 m^3 Pa K^{-1} mol^{-1}), S the chamber surface area (m^2), T the chamber air temperature (K) and $\delta C/\delta t$ is the gas concentration change over time (mol mol^{-1} s^{-1}). For flux calculations, only the concentration increases between 2 and 10 min after closure were used. Concentration increases were checked for non-linear trends and, if found, not used. Flux standard deviations were derived from the propagated standard deviations of the regression slope.

When homogeneity in footprint can be assured, micrometeorological and FC methods can be compared and used to study the role of photodegradation. Flux chambers can be shielded from incoming radiation, preventing photodegradation-induced carbon production, while micrometeorological methods capture all fluxes. Comparing the two methods therefore gives an indication of the presence and the magnitude of photodegradation-induced carbon fluxes (Rutledge et al., 2010). The use of this method was planned for our field experiment, but could not be applied due to lack of conformity between flux methods footprints, because of sparse photosynthetically active vegetation present in the footprint of the FG technique, causing the methods to be incomparable.

To study photodegradation, two different flux chambers, one with and one without solar radiation exposure, were used. During this experiment, the flux chambers were measuring six fixed chamber locations, chambers were manually moved every few days. One flux chamber was made opaque by use of light excluding aluminium foil (on 5 August). On the days before (28 July–5 August), all positions were compared by measuring the locations

with transparent chambers. On 3–5 August, the same locations were measured (with transparent chambers) as on 5–8 August, when one of the two chambers was covered. Both locations showed very similar CO_2 and CO flux patterns. Unfortunately, on 8 August, a leak has formed in the opaque chamber system, therefore direct comparison between the two treatments is limited to 3 days. Flux measurements made by the opaque chamber after 8 August are not shown. With blank measurements, the flux chambers were tested for internal CO_2 and/or CO production. No CO_2 production was found. Minor CO production was found during the day, negligible in comparison to field CO production: values presented in this paper are not corrected for this.

Studying thermal degradation-induced CO_2 production in the field is not possible due to the simultaneous temperature response of biological CO_2 production. For CO, no temperature dependent biological CO production is expected, wherefore measurement of thermal degradation-induced CO production in the field is possible. To study the role of thermal degradation in field CO exchange, chamber temperature sensors were installed, measuring air temperature every minute.

2.4 Laboratory experiment

Two different laboratory experiments were performed to study photo- and thermal degradation. Grass samples (senescent above ground grass material, mix of species as descibred in Methodology, pieces between 20-80 cm, not ground) for the laboratory experiment were taken from the field site. Mixed soil material samples were taken from the upper 3 cm of the soil, soil samples were not sieved. Both sample types were dried at 35 °C for 72h, to assure microbial activity to be negligible (Lee et al., 2012).

Photodegradation of senescent grass material was studied with a system consisting of a metal cylinder, inner diameter=6.5 cm, height=25 cm, area=33 cm^2, with an acrylic cap, which could be closed by screws. Transmittance of cap was measured: 0.2% (250 nm), 6.1% (260 nm), 35.9% (270 nm), 73.9% (280 nm), 89.6% (290 nm) and approximately 94% for larger wavelengths. The cylinder was placed beneath a UV-A and UV-B source (manufactor instrument: Isitec GmbH, Bremerhaven; UV-A lamp: Philips TL 60W/10R

(peak emission at 375 nm), UV-B lamp: Philips TL 40W/12RS (peak emission at 310 nm)). Radiation intensities at the sample location were quantified by use of an OceanOptics USB 2000 spectrometer with an optical fibre patch cord (P200-2-UV/VIS) and by an ILT1700 research radiometer with accompanying optical filters and are reported as comparison to natural radiation measured with the same instruments (determined in summer in Northern Germany, mid-day, no clouds, pointed at sun). Instrument radiation in the UV-A wavelength band 360-400 nm was measured to be 1.6 times higher than natural radiation, with the peak emission being at 375 nm (2.9 times natural radiation). Instrument radiation in the wavelength band 200-320 nm was measured to be 2.9 times higher than natural radiation, with the peak emission being between 290 and 310 nm (7.7 times natural radiation). During the experiment, different samples (empty cylinder, 2 gram-sample and 4 gram-sample) were exposed to different types/amounts of radiation (no radiation, UV-A and/or UV-B radiation). Grass in the cylinders was positioned so that at least 80% of the surface bottom was covered with grass material. During the experiments, air was continuously circulated from the cylinder to the FTIR and measured once per minute; emissions were derived from the measured concentration changes. Cylinder temperatures were monitored by an internal temperature probe (GTH 175/PT, Greisinger Electronics) and remained constant over the experiments (21, sd=0.15 °C). Every treatment was performed for 30 minutes and was duplicated.

To study thermal degradation, a glass flask (inner diameter= 6.7 cm, height=16 cm) was placed in a closed loop with the FTIR. For this experiment, only glass and stainless steel materials were used. 4 grass samples of 2 grams and 4 soil samples of 30 grams were taken. The grass sample was distributed equally in the flask. The soil sample was not sieved and filled approximately 1 cm (height) of the glass flask. The samples were heated in temperature steps of 5° (20–65 °C) by use of a controlled temperature water bath. Temperature time steps were 20 minutes. During the experiments, air was circulated from the glass flask to the FTIR and measured once per minute. After approximately 3 minutes, a stabilization in the CO production could be observed. Emissions were derived from the

measured concentration changes. Glass flask air temperatures were manually measured to check if water bath temperature was representative for grass and soil material temperatures; after 5 min, the glass flask air temperature had reached the same temperature as the water. All experiments were performed in duplicate and in dark conditions.

In the results sections, the given regression coefficients from polynomial fits are the explained sum of squares divided by the total sum of squares.

3 Results

During the field campaign (3 August–11 September, 2013), total precipitation was 15 mm and air temperatures ranged between 13 and 43 °C (see Fig. 2). Soil water content, measured at 10 cm depth was 18 % (VWC) and decreased less than 1 % over the experiment.

3.1 Flux measurements

FG CO_2 fluxes are shown in the Supplementary Materials. FG CO uptake (up to 1 nmol m^{-2} s^{-1}) and emission (up to 2 nmol m^{-2} s^{-1}) at night were measured (Fig 1). During the day, large ($\geq$ 10 nmol m^{-2} s^{-1}) CO emissions were recorded (Fig. 1). Based on the 31 days of FG measurements, on average net 42 nmol CO m^{-2} per day was estimated to be emitted.

FC CO_2 and FC CO fluxes of the transparent flux chamber can be seen in Fig. 2, rain events and incoming solar radiation are indicated. FC CO_2 fluxes showed a diurnal pattern with small emissions at night (1 µmol m^{-2} s^{-1}) and higher emissions during the day (up to 8 µmol m^{-2} s^{-1}). Large rain events on 20 and 27 August (6.6 and 2 mm) caused a short increase in chamber CO_2 fluxes. Locations without organic surface material (indicated as 'bare soils' in Fig 2) showed slightly lower CO_2 and CO fluxes.

At night, CO uptake of maximum 0.8 nmol m^{-2} s^{-1} was observed. During the day, emissions up to 3 nmol m^{-2} s^{-1} were observed. Over the course of the experiment, nightly CO uptake was continuously decreasing. The rain events caused a clear increase in nightly CO

uptake, after which the decreasing continued (Figs. 1 and 2). Based on 36 days of FC measurements, net on average net 8 nmol $CO\,m^{-2}$ per day was estimated to be emitted.

3.2 Photo- and thermal degradation

Photodegradation was studied by comparing opaque and transparent chamber measurements of three days (5–8 August) and by analysis of transparent FC data of a period in August (period with fixed location, stable weather conditions and no precipitation). Analysis of different periods (different locations with similar conditions) showed similar patterns.

Possible photo- and/or thermal degradation-induced CH_4 fluxes are not shown or evaluated here: FG CH_4 fluxes were too small for dependency analysis and CH_4 chamber fluxes mostly showed uptake, indicating a different process than photo- or thermal degradation.

3.2.1 CO_2 fluxes

Figure 3 shows the CO_2 fluxes (of transparent and opaque chamber) vs. air temperatures (Fig. 3a) and chamber temperatures (after 6 min closure, Fig. 3c). FC measurements showed very weak dependency on soil temperatures at 10 cm (data not shown). Blocking radiation showed no distinguished impact on measured CO_2 fluxes. Chamber CO_2 fluxes correlate well with air temperatures and less with chamber temperatures (Fig. 3a and c). Chamber coverage had an effect on chamber temperatures; during daytime hours, the opaque chamber temperature differed up to 10 °C from the transparent chamber temperature.

3.2.2 CO fluxes

A clear effect of chamber coverage on CO fluxes was visible; transparent chamber fluxes were higher during the day. FC CO fluxes correlate better with chamber temperatures than with air temperatures (Fig. 3b and d).

Figure 4 shows CO fluxes in the transparent chamber vs. air temperatures (Fig. 4a), chamber temperatures (after 6 min closure, Fig. 4b) and amount of solar radiation (Fig. 4c)

for a period in August. Again, CO fluxes relate best to chamber temperatures, and less to air temperatures and amount of incoming radiation (Fig. 4).

A temperature dependent biological CO uptake curve was fitted over chamber temperature data from (cold) night conditions (when abiotic fluxes are assumed to be minimal) and extrapolated to warmer temperatures. For biological CO uptake, a Q10-value from literature of 1.8 was chosen (Whalen and Reeburgh, 2001). An abiotic thermal degradation Q10-curve was fitted, also based on chamber temperature data, with a fitted Q10-value of 2.1. The sum of both processes agrees well the observed field CO fluxes ($R^2 = 0.85$, Fig. 5).

3.2.3 Laboratory experiment

In the laboratory, exposure of senescent plant material from the field site to high intensity UV-radiation did not result in increased CO_2 or CO fluxes in comparison to measurements performed in dark conditions (data shown in Supplementary Materials).

Grass and soil material samples exposed to different temperatures, under dark conditions, showed significant CO_2 production during lower temperatures ($< 40\,^{\circ}C$) and displayed small CO_2 emissions at higher temperatures ($> 55\,^{\circ}C$) (Fig. 6a). For CO, clear thermal production was found, exponentially increasing with higher temperatures (Fig. 6b). A Q10-value of 2.14 for senescest grass material and 2.00 for soil material was found to fit best to the observed laboratory thermal degradation CO fluxes (Fig. 6b).

4 Discussion

4.1 CO_2 fluxes

EC and FG measurements showed that the arid grassland was not yet in dormant state; significant CO_2 uptake was observed during the day (Fig. 7). FC CO_2 measurements, performed on locations without photosynthetic active vegetation, solely showed positive CO_2 fluxes, with peak emissions during the day up to $8\,\mu mol\,m^{-2}\,s^{-1}$. Figures 3a and 4a show

that CO_2 fluxes mostly relate to air temperatures, and poorly relate to soil temperatures (not shown). Expected is that most CO_2 production takes place close to the surface where the temperature follows air temperatures closer than it follows soil temperatures at 10 cm depth. In the ecosystem, the rain events resulted in an increase in CO_2 production for several days, showing the typical water-dependent response of arid ecosystem respiration (Fig. 2 and 7).

Photo- and thermal degradation

In the thermal degradation laboratory experiment, CO_2 production from senescest plant and soil material was observed during lower temperatures (20–40 °C), indicating remaining biological activity, even after drying. Above 50 °C, an increasing CO_2 production was observed with increasing temperatures, therefore expected to be (partly) of non-biological origin. Possible abiotic CO_2 production of approximately 3 $\mathrm{nmol\,min^{-1}\,gr^{-1}}$ for senescest grass material was observed. Extrapolating the thermal production rates of the senescent grass material to field conditions (assuming 200 gr of senescest plant material per m^2 at 55 °C), would result in a minor flux of 0.01 $\mathrm{\mu mol\,m^{-2}\,s^{-1}}$, in comparison to observed field fluxes of $> 1\,\mathrm{\mu mol\,m^{-2}\,s^{-1}}$. Based on the observations in the laboratory, it is expected that the soil material also produces thermal degradation-induced CO_2 fluxes. However, considering the relative cold and wet conditions of the *sub*surface soil material in the field, compared to laboratory conditions and to surface temperatures, it is expected that soil thermal degradation fluxes are minor in comparison to soil biological fluxes.

Other studies have observed thermal degradation-induced CO_2 fluxes with higher rates (approximately 125 $\mathrm{nmol\,CO_2\,gr^{-1}\,min^{-1}}$ for C3-grass at 55 °C), but also at lower temperatures (Lee et al., 2012). We can not verify this observation for our field material. Based on our observations, we propose that under *natural* conditions, when soil surface temperatures and especially soil subsurface temperatures rarely exceed 55 °C, thermal degradation-induced CO_2 fluxes do not play an important role in comparison to biological production, even in arid regions such as our study area.

We observed that chamber design can strongly influence chamber temperatures: during mid-day, the opaque and transparent chamber temperatures could differ up to 10 °C. As

observed in the laboratory experiment, *unnatural* high temperatures might lead to abiotic thermal CO_2 production. A research methodology aiming at measuring photodegradation can unintentionally result in high surface temperature levels, which could lead to unrepresentative high abiotic CO_2 production estimates.

The simultaneous use of opaque and transparent chambers was employed to study the effect of radiation on carbon fluxes in the field. Blocking radiation had no visible effect on field chamber CO_2 fluxes (Fig. 3a and c). CO_2 flux measurements performed on bare soil locations (soils without organic surface material) seemed lower than other locations; senescent surface material seemed to contribute to total CO_2 fluxes (Fig. 2b). However, only 3 days of bare soil measurements are available and no opaque chamber measurements on bare soil are present, therefore comparison is restricted.

The flux chambers, which were used to assess photodegradation, had a transparency of 90% or higher in the UV-B, UV-A and visible wavelength band. For our field experiment, we can therefore conclude that no large direct photodegradation fluxes (as suggested by Rutledge (2010) of 1 μmol m^{-2} s^{-1}) have been induced by natural sunlight intensities.
In the laboratory experiment, field site grass samples received above natural-intensity UV-radiation. In this experiment, no direct photodegradation fluxes were observed from field site grass material. While the laboratory experiment presented here does not prove that there are no photodegradation fluxes at all, the results from the laboratory experiment support the conclusion from the field experiment that *direct* photodegradation fluxes in arid ecosystems are not as important as suggested by a previous study (Rutledge et al., 2010).

The experiment was conducted on a field site situated in a Mediterranean climate. Based on annual precipitation and on measured respiration values, the ecosystem might seem too wet to be suitable to measure arid ecosystem processes. However, the climate is known for the precipitation free summers with high irradiation, causing the soil surface and surface materials to be fully dried out in summer. Since photodegradation is taking place at the soil surface, the ecosystem can be considered suitable for the assessment of this arid ecosystem process. The absolute amounts of possible photodegradation fluxes are

not influenced by the respiration fluxes. The expected rates of photodegradation fluxes (of 1 μmol m^{-2} s^{-1}, (Rutledge et al., 2010)) should have been detectable, even when mixed with respiratory fluxes.

Similar as what has been found by Kirschbaum et al. (2011); Lambie et al. (2014); Uselman et al. (2011), we did not observe the effects of photodegradation in field nor in the laboratory: no *direct* photodegradation-induced CO_2 fluxes have been observed. This is in contrast to other photodegradation studies, which have reported photodegradation fluxes in field (Rutledge et al., 2010) or in the laboratory (Lee et al., 2012). Potential explanations for this difference are: (a) the used field methodology in the previous study was not suitable for measuring direct abiotic degradation fluxes; (b) the role and significance of photodegradation differs per material and per field site; (c) studies might (partly) have misinterpreted thermal degradation fluxes as photodegradation fluxes or (d) photodegradation fluxes were too small to be observed by the presented method. We therefore do not question the existence of the photodegradation process, but doubt its suggested large role in arid ecosystems. However, as shown, the magnitude and the potential importance of thermal degradation-induced CO_2 fluxes in arid ecosystems are still unknown.

4.2 CO fluxes

During the measurement period, both CO uptake and emission have been observed by the FG method (patches of green active vegetation inside the footprint) as well as by the FC method (no photosynthetic active vegetation contributing to the fluxes) (Figs. 1 and 2). CO exchange measurements from FG and FC differed largely, most likely caused by the difference in footprint.

During the night, uptake of up to 1 nmol m^{-2} s^{-1} of CO was observed, which is most likely caused by microbial oxidation to CO_2 or CH_4 (Bartholomew and Alexander, 1979; Bruhn et al., 2013; Conrad, 1996; Ingersoll et al., 1974; Spratt and Hubbard, 1981; Yonemura et al., 2000; Whalen and Reeburgh, 2001). The CO uptake was decreasing over time but a rain event caused an enhanced uptake for some days (Figs. 1 and 2). Soil biota

being responsible for the CO uptake seems plausible since the effect of drought (decreasing uptake over time) and the effect of the rain (enhanced uptake) indicate a biological process. Nevertheless, with solely biological CO uptake taking place, one would expect higher uptake during warmer temperatures and no CO emission. It is expected that an abiotic process occurs simultaneously with the biotic uptake of CO, leading to a "buffering" effect on CO uptake. For this reason, CO deposition velocities could not be calculated.

Photo- and thermal degradation

We propose that the observed CO emissions in the flux chambers are caused by thermal degradation. FG measurements showed CO emissions during the day as well as during the night, indicating that CO is not (solely) produced by photodegradation (Fig. 1). By means of opaque chamber measurements, lower CO fluxes, in comparison to transparent chamber measurements, were detected. However, as described before, FC temperatures were strongly affected by the blocking of solar radiation. Analysis of CO fluxes showed a strong correlation with FC temperatures, and no relationship with radiation input, indicating that not the absence of radiation, but the indirect effect on temperature caused the lower CO emissions (Figs. 3 and 4).

FC CO fluxes were ranging between -1 and $2.5\,\mathrm{nmol\,m^{-2}\,s^{-1}}$ and only originated from soil or surface litter, since photosynthetic active vegetation was absent. Measured CO emissions are higher than reported for CO emissions from living plants and similar to values found for senescest plant material (Bruhn et al., 2013; Derendorp et al., 2011; Lee et al., 2012; Schade et al., 1999; Zepp et al., 1998). However, the measurements are a cumulative signal of uptake and emission and can therefore not be compared directly to other studies.

In the laboratory experiment, where grass from the field site was exposed to above natural intensity UV-radiation, no photodegradation-induced CO fluxes were observed. However, significant thermal degradation-induced fluxes from the senescest grass and soil material were measured, even measureable at low temperatures (20 °C). At 50 °C, a thermal CO pro-

duction rate of senescest grass material of 0.13 $\mathrm{nmol\,min^{-1}\,gr^{-1}}$ was found. Extrapolating this observation to field conditions (assuming 200 grams of senescest plant material per $\mathrm{m^2}$ at 50 °C), would result in a flux of approximately 0.4 $\mathrm{nmol\,m^{-2}\,s^{-1}}$, which is approximately 5 times lower than the net measured field CO fluxes. Extrapolating the thermally-induced CO production rate of the soil material to field conditions would result in an estimated production of approximately 1 $\mathrm{nmol\,m^{-2}\,s^{-1}}$ from the upper 3 cm of the soil during a summer day. However, while this estimate indicates that abiotic thermal soil CO production indeed might play a major role, for accurate estimates for net soil CO uptake or emission, more information about biological CO uptake and about the soil profile is needed.

The observed field chamber CO fluxes are suggested to be a cumulative signal of biological uptake and abiotic thermal degradation. Both processes were fitted over chamber temperatures. For the fitting of biological CO uptake, a Q10-value of 1.8 was chosen (Whalen and Reeburgh, 2001). To match the cumulative measured CO fluxes (purple diamonds in Fig. 5), a higher Q10-value of 2.1 for the abiotic thermal soil CO production was fitted ($R^2 = 0.85$).

The laboratory measurements were used to *experimentally* determine the Q10-value of thermal degradation-induced CO fluxes. Q10-values of 2.14 for senescent grass and 2.00 for soil material were measured. These values are similar to the Q10-value which was fitted for the thermal degradation process to match the cumulative field measurements, as described in the previous paragraph (Fig. 5).

The soil CO uptake process, taking place below the surface, is subject to buffered chamber temperatures, and therefore the chosen Q10-value might be an underestimation. Also, the biological soil uptake is not expected to follow the Q10-temperature response at higher temperatures ($> 35\,°\mathrm{C}$). Nevertheless, the difference in temperature response (as a consequence of different Q10-values or as a consequence of buffered temperatures) causes biological CO uptake to be dominant during colder (chamber) temperatures, and thermal degradation to be dominant during warmer (chamber) temperatures. During our field experiment, thermal degradation started to be dominant from approximately 25 °C (chamber temperature) and followed an exponentional curve with higher temperatures

(Fig. 5).

The temperatures inside the chamber were higher than the temperatures outside the chamber. Although this will result in higher fluxes inside the chamber compared to the ecosystem around it, the correlation between temperatures inside the chamber and the CO flux should be representative for the ecosystem. The laboratory study shows a similar relationship between temperature and CO flux. According to our results, the temperatures outside the chamber are high enough to induce significant thermal degradation fluxes. This is supported by the measured CO fluxes by the FG technique. FG CO emissions were higher, likely due to its footprint which contained relatively more dead vegetation (thermal degradating material) since, for practical reasons, the chambers were placed over lower dead vegetation. Also, the FG footprint contained active vegetation, which is another possible CO emitting source (Bruhn et al., 2013).

Overall, the measurements show that the field site is a net source of CO during the summer months, affecting the atmospheric chemistry, at least at plant level, via OH^- depletion. More field measurements on annual CO exchange are needed to better understand the role of thermal degradation in CO and CO_2 exchange in arid regions.

5 Conclusions

In our field and laboratory experiment, direct photodegradation-induced CO_2 and CO fluxes have not been observed. Based on laboratory experiments, the production of thermal degradation-induced CO_2 is expected, but only significant under unnaturally high temperatures. In the laboratory, thermal degradation-induced CO fluxes were clearly observed, also at relatively low temperatures (20 °C). In the field, biological CO uptake as well as abiotic CO production was observed; abiotic CO production is assumed to be mainly a product of thermal degradation. The Q10-value of the CO producing thermal degradation process,

as determined in the laboratory, agrees well with the fitted Q10-value for abiotic CO fluxes measured at the field site.

Not all litter types are reported to be sensitive to photodegradation, which could explain why we did not measure photodegradation-induced fluxes. Also, we realize that in field conditions, partitioning photodegradation from thermal degradation or biological processes is challenging and minor photodegradation fluxes might not be detectable. We therefore do not exclude the existence of photodegradation. However, in our field experiment in an arid ecosystem, we were not able to observe any direct photodegradation-induced carbon fluxes, showing that direct photodegradation does not play a major role in this arid ecosystem. Previous studies suggesting the occurrence of major photodegradation fluxes might possibly have neglected thermal degradation fluxes, which is an indirect effect of radiation. The potential importance of abiotic decomposition in the form of thermal degradation, especially for arid regions, should be considered and be studied in more detail.

Acknowledgements. We are grateful for the support of InGOS (European Communitiy Seventh Framework Programme (FP7/2007-2013)) for funding the field experiment. Also, we would like to thank TTorch who supported the author in an exchange stay at University of Tuscia (TTORCH ESF Exchange Grant, part of the ESF "Tall Tower and Surface Research Network for Verification of Climate Relevant Emissions of Human Origin"-project). We would also like to thank the ESSReS Research School, part of the Helmholtz Centre for Polar and Marine Research. We thank Alessio Boschi, Michele Tomassucci and Sipko Bulthuis for their help during the field experiment. Furthermore, we would like to thank Tommaso Chiti for his help taking the soil samples, Stefano Ponziani for providing field data and Annika Wieferich for her additional experiments in the laboratory. Thanks is also extended to the two anonymous reviewers whose comments helped improve our manuscript.

6 Supplementary materials

Flux Gradient method

FG measurements were performed once per hour. Air inlet heights were at 1.3 and 4.2 m. Air was sampled at 1 L min^{-1}. Sampling lines of stainless steel were used for the experi-

ment. For 30 min h^{-1}, the airflows were led to air sampling bags, after that the bag inlet was closed until analysis. Before the analysis, the FTIR measurement cell was evacuated and flushed twice with measurement air before being filled. Per air sample, a 3 min-spectra (static) measurement was taken. FG measurements were performed at the same point as of the EC set-up (measurement height at 3.5 m). During day time, footprint analysis showed that 90 % of the source area of the EC signal came from the grassland area within 150 m. Since the FG method is measuring at the same location and height, it is expected that daytime FG fluxes mainly originate from the grassland area as well. During nighttime, footprint analysis showed fluxes mainly originating from outside the grassland. FG CO_2 fluxes agreed well with EC fluxes and ranged between -7 and 8 µmol m^{-2} s^{-1} (Fig. 7)
By using the FG method, fluxes can be calculated by:

$$F = K\frac{\delta C}{\delta z} \tag{2}$$

wherein δC is the difference in concentration of a gas species (mol m^{-3}) between the two inlet-heights (δz (m)) and K is the diffusion coefficient (m^2 s^{-1}), and F the flux (mol m^{-2} s^{-1}). K can be parameterized using the data of a sonic anemometer, based on the friction velocity (u-star), the Von Karman-constant, the effective height and the stability factor (ζ) (Foken, 2006).

Laboratory photodegradation experiment

CO_2 and CO grass sample emission was measured under dark and UV-radiation conditions and compared to blank measurements (Figure 8). In comparison to blank measurements, no positive influence of UV-radiation was found on CO_2 and CO production. Observed emissions under UV-radiation were slightly smaller than in dark conditions, which could be caused by the inhibiting effect of UV-radiation on microbial decomposition (Lambie et al., 2014). However, differences were not significant.
Rutledge (2010) estimated photodegradation fluxes of 1 μmol CO_2 m^{-2} s^{-1} in sunny conditions (60000 nmol CO_2 m^{-2} min^{-1}). Considered are the following assumptions.
80% of fieldsite surface is covered with dry organic matter. 80 % of laboratory surface

is covered with dry organic matter. Expected is that at least 50% of photodegradation is caused by UV-radiation. The laboratory samples received 2 times more UV-radiation than under natural conditions. Sample rates are measured over 0.0033 m^{-2} (33 cm^{-2}). Based on Rutledge (2010), the following emission magnitudes were therefore expected in the laboratory experiment: 60000x0.5x2x0.0033=200 nmol CO_2 min^{-1} per sample.

Schade (1999) measured approximately 250 nmol CO m^{-2} min^{-1} (250*10^9 molecules cm^{-2} s^{-1}) of photodegradation fluxes under peak daytime radiation. Considering the same assumptions, then CO emissions with a magnitude of 250x0.5x2x0.0033=8.3 nmol m^{-2} min^{-1} per sample were expected. Calculated expected productions are indicated in Figure 8.

References

Austin, A. T. and Ballaré, C. L.: Dual role of lignin in plant litter decomposition in terrestrial ecosystems, P. Natl. Acad. Sci. USA, 107, 4618–4622, 2010.

Austin, A. T. and Vivanco, L.: Plant litter decomposition in a semi-arid ecosystem controlled by photodegradation, Nature, 442, 555–558, 2006.

Bartholomew, G. and Alexander, M.: Microbial metabolism of carbon monoxide in culture and in soil., Appl. Environ. Microb., 37, 932–937, 1979.

Brandt, L., King, J., Hobbie, S., Milchunas, D., and Sinsabaugh, R.: The role of photodegradation in surface litter decomposition across a grassland ecosystem precipitation gradient, Ecosystems, 13, 765–781, 2010.

Bruhn, D., Mikkelsen, T. N., Øbro, J., Willats, W. G. T., and Ambus, P.: Effects of temperature, ultraviolet radiation and pectin methyl esterase on aerobic methane release from plant material, Plant Biol., 11, 43–48, 2009.

Bruhn, D., Albert, K. R., Mikkelsen, T. N., and Ambus, P.: UV-induced carbon monoxide emission from living vegetation, Biogeosciences, 10, 7877–7882, doi:10.5194/bg-10-7877-2013, 2013.

Conrad, R.: Soil microorganisms as controllers of atmospheric trace gases (H_2, CO, CH_4, OCS, N_2O, and NO), Microbiol. Rev., 60, 609–640, 1996.

Conrad, R. and Seiler, W.: Role of microorganisms in the consumption and production of atmospheric carbon monoxide by soil, Appl. Environ. Microb., 40, 437–445, 1980.

Conrad, R. and Seiler, W.: Arid soils as a source of atmospheric carbon monoxide, Geophys. Res. Lett., 9, 1353–1356, 1982.

Derendorp, L., Quist, J., Holzinger, R., and Röckmann, T.: Emissions of H_2 and CO from leaf litter of *Sequoiadendron giganteum*, and their dependence on UV radiation and temperature, Atmos. Environ., 45, 7520–7524, 2011.

Foken, T.: Angewandte Meteorologie, Springer, Berlin, Heidelberg, 2006.

Formánek, P., Rejšek, K., and Vranová, V.: Effect of elevated CO_2, O_3, and UV radiation on soils, The Scientific World Journal, 730149, doi:10.1155/2014/730149, 2014.

Friedlingstein, P., Cox, P., Betts, R., Bopp, L., Von Bloh, W., Brovkin, V., Cadule, P. Doney, S., Eby, M., Fung, I., Bala, G.,John, J.,Jones, C., Joos F., Kato, T., Kawamiya, M., Knorr, W., Lindsay, K., Matthews, H. D., Raddatz, T., Rayner, P., Reick, C., Roeckner, E., Schnitzler, K.-G., Schnur, R., Strassman, K., Weaver, A. J., Yoshikawa, C., and Zeng, J.: Climate-carbon cycle feedback analysis: Results from the C4MIP model intercomparison, J. Climate, 19, 3337–3353, 2006.

Funk, D. W., Pullman, E. R., Peterson, K. M., Crill, P. M., and Billings, W.: Influence of water table on carbon dioxide, carbon monoxide, and methane fluxes from taiga bog microcosms, Global Biogeochem. Cy., 8, 271–278, 1994.

Griffith, D. W. T., Deutscher, N. M., Caldow, C., Kettlewell, G., Riggenbach, M., and Hammer, S.: A Fourier transform infrared trace gas and isotope analyser for atmospheric applications, Atmos. Meas. Tech., 5, 2481–2498, doi:10.5194/amt-5-2481-2012, 2012.

Hammer, S., Griffith, D. W. T., Konrad, G., Vardag, S., Caldow, C., and Levin, I.: Assessment of a multi-species in situ FTIR for precise atmospheric greenhouse gas observations, Atmos. Meas. Tech., 6, 1153–1170, doi:10.5194/amt-6-1153-2013, 2013.

Ingersoll, R., Inman, R., and Fisher, W.: Soil's potential as a sink for atmospheric carbon monoxide, Tellus, 26, 151–159, 1974.

King, J. Y., Brandt, L. A., and Adair, E. C.: Shedding light on plant litter decomposition: advances, implications and new directions in understanding the role of photodegradation, Biogeochemistry, 111, 57–81, 2012.

Kirchhoff, V. W., Da Silva, I., and Browell, E. V.: Ozone measurements in Amazonia: dry season versus wet season, J. Geophys. Res.-Atmos., 95, 16913–16926, 1990.

Kirschbaum, M. U., Lambie, S. M., and Zhou, H.: No UV enhancement of litter decomposition observed on dry samples under controlled laboratory conditions, Soil Biol. Biochem., 43, 1300–1307, 2011.

Kisselle, K. W., Zepp, R. G., Burke, R. A., de Siqueira Pinto, A., Bustamante, M., Opsahl, S., Varella, R. F., and Viana, L. T.: Seasonal soil fluxes of carbon monoxide in burned and unburned Brazilian savannas, J. Geophys. Res.-Atmos., 107, LBA–18, 2002.

Lal, R.: Carbon sequestration in dryland ecosystems, Environ. Manage., 33, 528–544, 2004.

Lambie, S., Kirschbaum, M., and Dando, J.: No photodegradation of litter and humus exposed to UV-B radiation under laboratory conditions: No effect of leaf senescence or drying temperature, Soil Biol. Biochem., 69, 46–53, 2014.

Lee, H., Rahn, T., and Throop, H.: An accounting of C-based trace gas release during abiotic plant litter degradation, Glob. Change Biol., 18, 1185–1195, 2012.

Lin, Y. and King, J. Y.: Effects of UV exposure and litter position on decomposition in a California Grassland, Ecosystems, 17, 158–168, 2014.

Rutledge, S., Campbell, D. I., Baldocchi, D., and Schipper, L. A.: Photodegradation leads to increased carbon dioxide losses from terrestrial organic matter, Glob. Change Biol., 16, 3065–3074, 2010.

Schade, G. W., Hofmann, R.-M., and Crutzen, P. J.: CO emissions from degrading plant matter, Tellus B, 51, 889–908, 1999.

Smith, W. K., Gao, W., Steltzer, H., Wallenstein, M., and Tree, R.: Moisture availability influences the effect of ultraviolet-B radiation on leaf litter decomposition, Glob. Change Biol., 16, 484–495, 2010.

Spratt, H. G. and Hubbard, J. S.: Carbon monoxide metabolism in roadside soils, Appl. Environ. Microb., 41, 1192–1201, 1981.

Stocker, T. F., Qin, D., Plattner, G.-K., Tignor, M., Allen, S. K., Boschung, J., Nauels, A., Xia, Y., Bex, V., and Midgley, P. M.: Climate change 2013: The Physical Science Basis, Intergovernmental Panel on Climate Change, Working Group I Contribution to the IPCC Fifth Assessment Report (AR5), Cambridge Univ. Press, New York, 2013.

Tarr, M. A., Miller, W. L., and Zepp, R. G.: Direct carbon monoxide photoproduction from plant matter, J. Geophys. Res.-Atmos., 100, 11403–11413, 1995.

Throop, H. L. and Archer, S. R.: Interrelationships among shrub encroachment, land management, and litter decomposition in a semidesert grassland, Ecol. Appl., 17, 1809–1823, 2007.

Throop, H. L. and Archer, S. R.: Resolving the dryland decomposition conundrum: some new perspectives on potential drivers, in: Progress in Botany, Springer, Berlin, Heidelberg, 171–194, 2009.

Uselman, S. M., Snyder, K. A., Blank, R. R., and Jones, T. J.: UVB exposure does not accelerate rates of litter decomposition in a semi-arid riparian ecosystem, Soil Biol. Biochem., 43, 1254–1265, 2011.

Vigano, I., van Weelden, H., Holzinger, R., Keppler, F., McLeod, A., and Röckmann, T.: Effect of UV radiation and temperature on the emission of methane from plant biomass and structural components, Biogeosciences, 5, 937–947, doi:10.5194/bg-5-937-2008, 2008.

Whalen, S. and Reeburgh, W.: Carbon monoxide consumption in upland boreal forest soils, Soil Biol. Biochem., 33, 1329–1338, 2001.

Williamson, C. E., Metzgar, S. L., Lovera, P. A., and Moeller, R. E.: Solar ultraviolet radiation and the spawning habitat of yellow perch, *Perca flavescens*, Ecol. Appl., 7, 1017–1023, 1997.

Yonemura, S., Kawashima, S., and Tsuruta, H.: Carbon monoxide, hydrogen, and methane uptake by soils in a temperate arable field and a forest, J. Geophys. Res.-Atmos., 105, 14347–14362, 2000.

Zepp, R. G., Callaghan, T., and Erickson, D.: Effects of enhanced solar ultraviolet radiation on biogeochemical cycles, J. Photoch. Photobio. B, 46, 69–82, 1998.

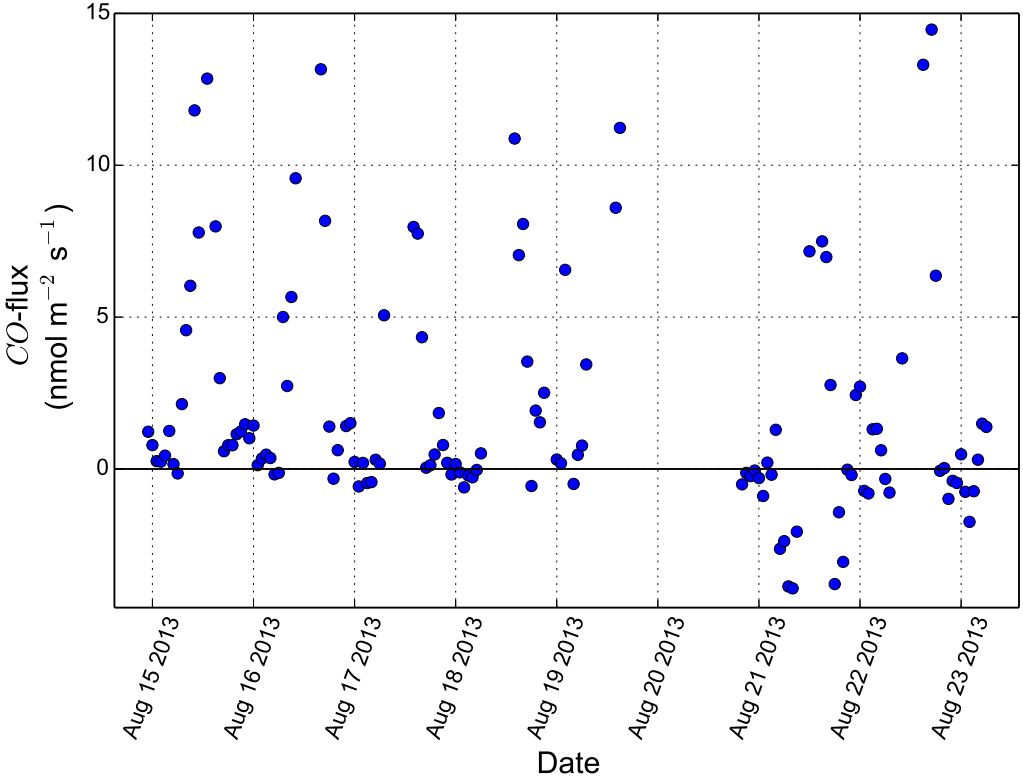

Figure 1. Flux Gradient CO measurements over 8 days in August. A large rain event took place on 20 August.

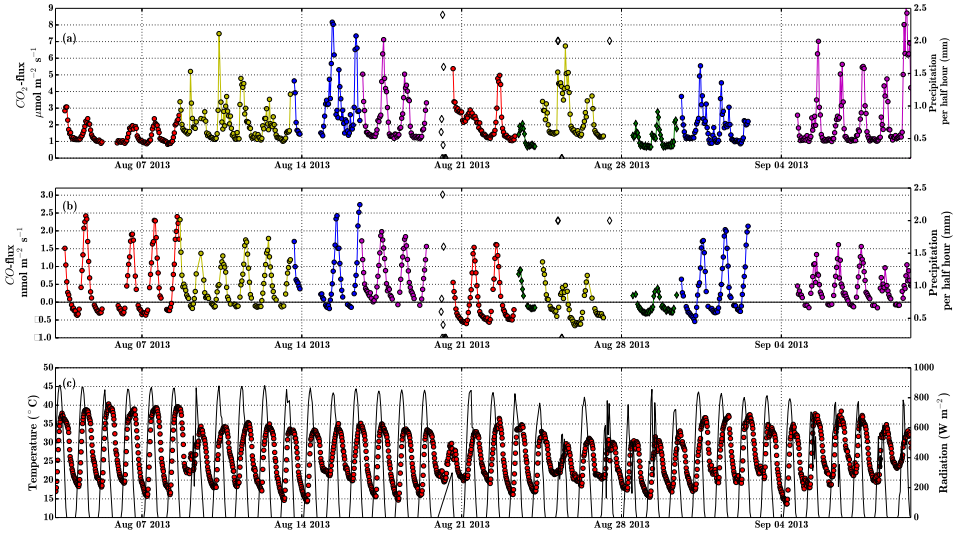

Figure 2. (a, b) Chamber CO_2 and CO fluxes with (errorbars with SD of flux are included but not visible due to low value) during field experiment, different colors are different locations. The two bare soil locations (soils without organic surface material) are both presented with green diamonds. Rain events (open diamonds) are indicated. Presented data is from transparent flux chamber measurements; **(c)** Air temperature (°C) (red circles) and radiation (W m^{-2}) (black line).

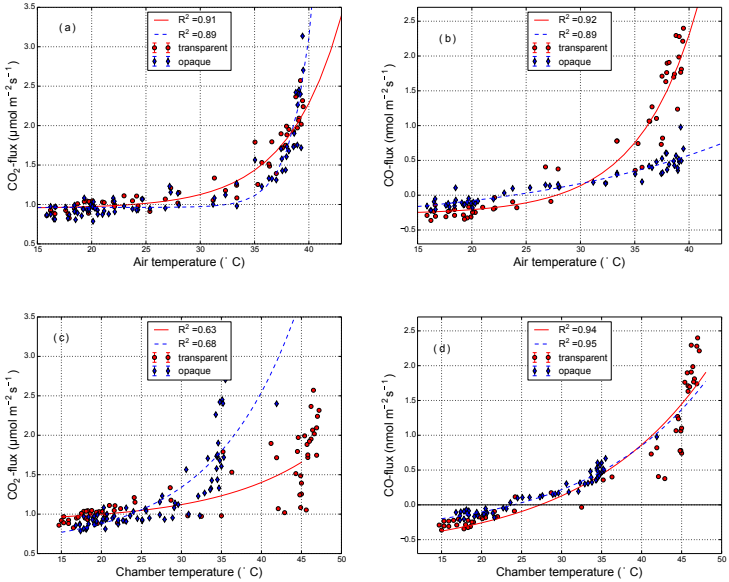

Figure 3. Transparent and opaque flux chamber CO_2 fluxes (left) and CO fluxes (right) vs. air temperature **(a, b)** and chamber temperature after 6 min closure **(c, d)**. Regression coefficients of polynomial fits are given in the legends.

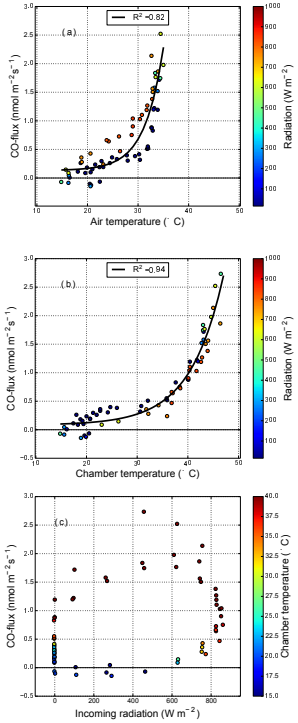

Figure 4. Transparent flux chamber CO fluxes for 15–19 August vs. air temperature **(a)**, chamber temperature after 6 min closure **(b)** and solar radiation **(c)**. Regression coefficients of polynomial fits are given in the legends.

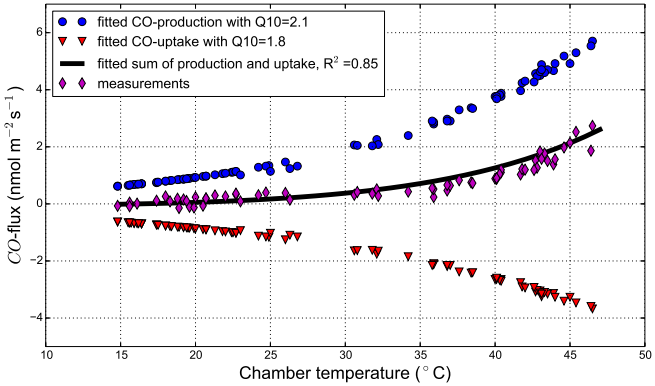

Figure 5. Fitted CO fluxes for 15–19 August (black line) for measured field CO fluxes (purple diamonds)($R^2 = 0.85$). The cumulative fitted CO flux is a sum of fitted CO uptake (with Q10 = 1.8, based on literature (Whalen and Reeburgh, 2001) and fitted CO production (with Q10 = 2.1) based on chamber temperature (after 6 min closure).

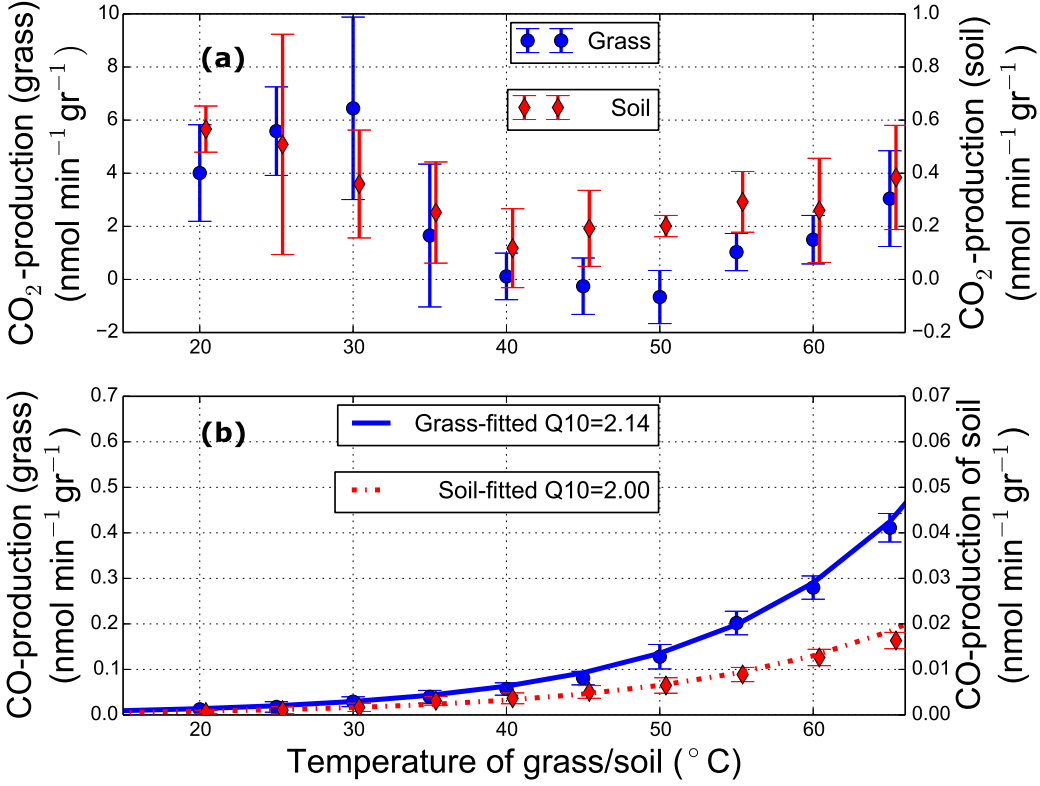

Figure 6. (a) Average CO_2 production of grass and soil material (nmol min^{-1} gr^{-1}) over different temperatures in the laboratory experiment; **(b)** Average CO production of grass and soil material (nmol min^{-1} gr^{-1}) over different temperatures in the laboratory experiment, with fitted Q10-value.

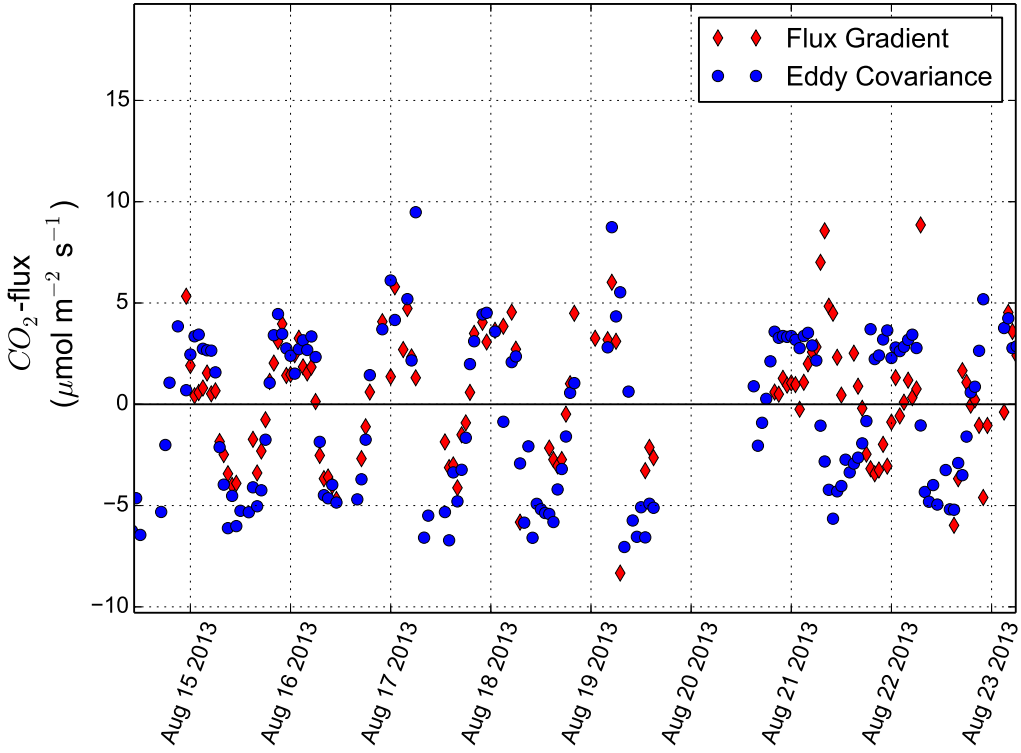

Figure 7. Comparison of Flux Gradient- and Eddy Covariance-CO_2 flux measurements over 8 days in August. On 20 August was a large rain event.

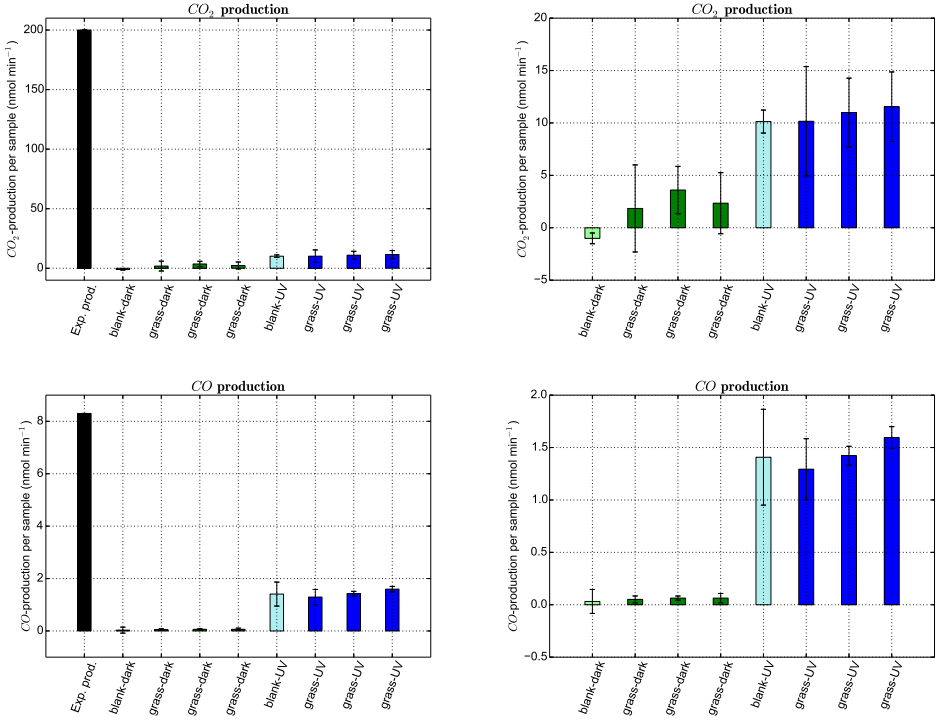

Figure 8. Results of photodegradation laboratory experiment. Results are for 2 gram samples, placed in a 33 cm^2 cylinder. Upper figures: CO_2 production under different treatments. Exp. prod. stands for expected production based on comparison to Rutledge (2010). Right figure is zoom-in of left figure. Lower figures: CO production under different treatments. Exp. prod. stands for expected production based on comparison to Schade (1999). Right figure is zoom-in of left figure.